Tailored High Performance Shape Memory Epoxy-Silica Nanocomposites. Structure Design

Journal:	*Polymer Chemistry*
Manuscript ID	PY-ART-09-2015-001450.R1
Article Type:	Paper
Date Submitted by the Author:	26-Oct-2015
Complete List of Authors:	Matejka, Libor; Institute of Macromolecular Chemistry, Department of Polymer Networks + Mechanical Properties Ponyrko, Sergii; Institute of Macromolecular Chemistry, AS CR, Nanostructured Polymers and Composites Donato, Ricardo; Universidade Federal do Rio Grande do Sul,

Journal Name

ARTICLE

Tailored High Performance Shape Memory Epoxy-Silica Nanocomposites. Structure Design.

Received 00th January 20xx,
Accepted 00th January 20xx

DOI: 10.1039/x0xx00000x

www.rsc.org/

S. Ponyrko[a], R. K. Donato[a,b] and L. Matějka*[a]

The high performance shape memory (SM) epoxy-silica nanocomposites have been synthesized. The structure of the corresponding SM polymer was designed on the basis of the determined relationships between structure, mechanical properties and SM performance. The recovery stress, as a crucial SM property of high performance systems, is governed by the material toughness while the efficiency of the SM performance is controlled by morphological homogeneity and viscoelastic behaviour of the polymer as well as by experimental conditions of the SM procedure. The nanocomposites were prepared by *in situ* generation of nanosilica in the epoxy matrix. The non-aqueous sol-gel procedure was applied and the ionic liquid (IL) was used at synthesis as a multifunctional agent controlling morphology and mechanical properties. The effect of nanosilica, IL, crosslinking density of the epoxy network, physical crosslinking as well as application of the concept of bimodal networks on SM performance was evaluated and discussed. Based on the knowledge of the corresponding relationships and structural effects the SM nanocomposite was synthesized showing the high recovery stress σ_r = 3.9 MPa or high deformability ε_b = 103 %. The study contributed to the better understanding of the SM behaviour of polymers.

1. Introduction

Shape-memory polymers (SMP) are an important class of smart polymers capable to memorize their shape. After a mechanical deformation and fixing a temporary shape they recover the original permanent shape upon external stimulation.[1,2] The recovery can be triggered by heat, light, electric or magnetic field, etc. The thermal-responsive SMPs are the most studied systems and will be the focus of this paper. In past 10 years a remarkable advance in stimuli responsive SMPs was achieved providing the potential applications in medical, aerospace, civil engineering, energy, and bionics areas.

The SMPs are composed of two phases – a permanent one and a switching phase which is sensitive to an external stimulus. The permanent phase, maintaining the dimensional stability, is chemical or physical network. The switching phase enables a reversible transformation between hard and soft/liquid states. The most typical are the glassy and crystalline states serving to fix the temporary shape of a polymer. Thermally induced transformation of the switching phase, i.e. glass transition or melting, then leads to recovery of the original shape.

The shape memory (SM) properties of polymers are usually tested by the thermal SM cycle. It consists of (i) heating the sample above transformation temperature (T_{trans}), corresponding to T_g or T_m, up to deformation temperature T_d, (ii) deforming the sample into a temporary shape, (iii) cooling the sample below T_{trans} down to the setting temperature T_s while maintaining the deformation load; the temporary shape is quenched by vitrification or crystallization, (iv) the deformation load is released, (v) re-heating the sample above T_{trans} up to T_d. This step leads to a recovery to the original shape under nonconstrained conditions or to a stress recovery at constrained conditions, i.e. the sample is fixed at constant length. The SM behaviour of a SMP is characterized by the quantities, such as shape fixity R_f, shape recovery R_r, rate of recovery V_r and recovery stress σ_r. The first one indicates the ability of a polymer to fix the temporary shape after cooling and unloading, R_r and V_r describe the capacity of the material to recover the original shape and σ_r is a stress generated at the constrained recovery.[3] Generally, the high shape fixity requires a high modulus at setting temperature, G_s, and scales with the expression (1 - G_r/G_s), while the recovery is related mainly to the rubbery modulus G_r. The recovery stress increases with increasing G_r, and the nonconstrained recovery is faster at low G_r. Also broadness of the thermal transition plays a role. The sharp transition makes prompt fixing the shape at cooling and triggering shape recovery at heating.

The typical SMPs are based on polyurethanes[4], polyolefines[5], acrylates[6], polystyrene-based polymers[7] or epoxies[8]. With respect to another common shape memory material, shape memory alloys (SMA)[9,10], the SMPs are beneficial due to their variability, easier processability and larger attainable strain. The recoverable strain up to 700% has been reported at SMPs

[a] Institute of Macromolecular Chemistry, Academy of Sciences of the Czech Republic, Heyrovsky Sq. 2, Prague, Czech Republic. E-mail: matejka@imc.cas.cz
[b] Laboratory of Technological Processes and Catalysis, Institute of Chemistry, Universidade Federal do Rio Grande do Sul, Av. Bento Goncalves 9500, Porto Alegre-RS, Brazil

based on physically crosslinked thermoplastics.[4] However, the physical networks are prone to creep and irreversible plastic deformation resulting in a low shape fixity and recovery.[11] Therefore, covalently crosslinked networks, thermosets, are considered as more perspective shape memory candidates. They show a better shape fixity and recovery as well as a higher thermal and chemical stability. In general, however, the SMPs exhibit a low mechanical strength and stiffness resulting in poor SM properties such as a low recovery stress, being σ_r < 3 MPa and rate of recovery compared to SMA. This drawback has largely restricted the applications of SMPs.

The epoxy based materials are known to display superior mechanical properties. Moreover, a low curing shrinkage, versatile chemistry of curing and easy adjustable thermomechanical properties make the epoxy based glassy thermosets perspective SM materials, displaying the excellent shape fixity and recovery, reaching 95 - 100%.[12] Despite their beneficial properties, however, not too many teams deal with the epoxy based SMPs due to a low deformability and high T_g of the corresponding systems.[13-19] Rousseau and Xie[20] studied the effect of epoxy network structure on shape memory properties in order to give guidelines for use of epoxy systems as high-performance SMP. They investigated the networks of different crosslinking density and flexibility by using different amine crosslinkers or introducing the monoamine, and applying both aromatic and aliphatic epoxies. In this way, T_g and the rubbery modulus of networks were tuned in a wide range. However, the SM behaviour was found to be independent of a network structure, composition, crosslink density and viscoelasticity. All systems showed excellent SM performance with shape fixity and shape recovery approaching 100%. Only very slight differences were determined unveiling that SM properties decline at a low crosslinking density and a high chain flexibility. The recovery stress, however, was not reported.

The drawback of the epoxy-based SMP consists in a low deformability: elongation at break ε_b < 30%, which limits their potential application. Several ways of increasing their deformability were reported. Gall et al. used the procedure of deformation at T close T_g instead in the rubbery state.[21] This strategy makes it possible to increase ε_b from 30% to ca. 60%.[20] However, shape fixity was noticeably reduced. Williams et al.,[22] described the SMP epoxy system with pendant alkyl chains undergoing self-assembling by tail-to-tail association thus forming physical crosslinks. This, partially physically crosslinked SMP showed deformability ε_b as high as 75%. Highly deformable epoxy-based SMP has been recently investigated by Xie et al.[23] The composition of the networks based on the diepoxide E44 and Jeffamine D230 was tuned by varying stoichiometry ratio epoxy/amine controlling thus the network crosslinking density. The networks of a low crosslinking density, at a high amine excess, were extended up to ε_b = 111 and 212%, at rubbery state and at $T \sim T_g$, respectively. Despite the low crosslink density, the systems showed the perfect shape fixity, R_f > 99% and recovery ratio, R_r = 97 - 99.4%. The stress recovery was not reported. However, the deformability increased at the expense of stiffness and the modulus was reduced by 360% implying likely a severe decline of σ_r.

In order to overcome the main drawback of SMPs, a low stiffness, strength and a low recovery stress, the attention has been paid to the polymer reinforcement. The polymer fillers are able to improve the mechanical performance and shape recovery stress of SMPs[24-27] and consequently the polymer composites/nanocomposites are perspective materials for SM systems.[28-31] Different types of reinforcing agents were used, such as exfoliated nanoclay[32], microfibers[33], carbon nanotubes[34], functionalized SiO_2 particles[35] enhancing mechanical and SM properties. Beloshenko et al.[36], revealed an importance of strength of a polymer-filler interphase. The composites with the strong polymer-silica and weak polymer-expanded graphite interactions displayed recovery stress σ_r = 1.1 and 0.6 MPa, respectively. Gall et al.[37] described the fabrication and characterization of the epoxy-based SMP composites filled with nanoparticulate SiC. The modulus was enhanced and the recovery force in the nanocomposites was shown to increase by 50% with the addition of 20 wt. % SiC. At a high content of nanofiller, however, a permanent deformation occurred deteriorating the SM properties. Just the permanent deformation and a decrease in attainable strain limit the application of composites/nanocomposites as a SM material.

In this work we aim to prepare and study the high performance epoxy-based SMP showing the high recovery stress and a high deformability, while keeping an excellent shape fixity and recovery. The study is focused on design of structure of the SMP and determination of relationships between structure and SM properties of the investigated systems. The structural design makes it possible to control the thermomechanical, tensile mechanical and viscoelastic properties and thereby to optimize the SM behavior. We have investigated the reinforced systems, epoxy-silica nanocomposites, in order to enhance mechanical properties. The nanocomposites are more efficient than the classical composites due to a large interfacial area and a correspondingly stronger polymer-nanofiller interaction. The structure design takes into account (i) structure of the epoxy matrix including crosslinking density of the network, flexibility of polymer chains, physical crosslinking, as well as a concept of bimodal networks, (ii) the nanocomposite morphology involving nanofiller content and quality of dispersion in matrix as well as an interphase interaction. In addition to the material structure design also the optimization of a SM procedure was performed in order to fully exploit a potential of SMP materials.

The special approach has been applied for synthesis of the epoxy-silica nanocomposites in order to tune their structure and morphology to be most suitable for the SMP system. The different types of epoxy-amine networks based on diglycidylether of Bisphenol A (DGEBA) were used as polymer matrices. The nanocomposites were prepared by *in situ* generation of nanosilica in the epoxy network ensuring thus a good dispersion of nanofiller in the matrix. The non-aqueous sol-gel process was used to incorporate nanosilica. This

procedure enables a better control of the nanocomposite morphology and a more efficient enhancement of mechanical properties compared to the classical aqueous sol-gel procedure.[38,39] In addition, absence of water makes the synthesis easier. Moreover, the ionic liquids (ILs) were applied at synthesis making possible modification of morphology and further homogenization by improvement of interaction polymer-nanosilica, as well as reinforcement of the nanocomposite.[40,41]

Novelty of this paper consists in the design and synthesis of high performance SMPs by application of epoxy-silica nanocomposites with well controlled structure and thermomechanical properties using a non-aqueous sol-gel process under catalytic action of the ILs. The general relationships between the nanocomposite structure and SM properties were determined providing thus better understanding of the SM behaviour.

2. Experimental

2.1. Materials

Diglycidyl ether of Bisphenol A (DGEBA, n = 0.17) based resin with the equivalent weight of the epoxy groups E_E = 187 gmol^{-1} epoxy groups was obtained from the Aldrich.

Crosslinking agents: poly(oxypropylene)diamines - Jeffamine® D230 and D400 were received from BASF, Ethylenediamine (EDA) and 4,4′-Methylenebis(3-methylcyclohexylamine) (Laromin) were obtained from Aldrich, the polyether monoamines Jeffamine® M600 and M1000 were purchased from Hunstman, Amine-terminated butadiene-acrylonitrile copolymer (Hycar ATBN 1300x16) was obtained from Nanoresis.

Inorganic components: tetramethoxysilane (TMOS) was purchased from Fluka. Borontrifluoride monoethylamine (BF_3MEA) was obtained from the Aldrich.

The ionic liquids 1-decyl-3-methylimidazolium tetrafluoroborate ($C_{10}BF_4$), 1-butyl-3-methylimidazolium tetrafluoroborate (C_4BF_4) and 1-butyl-3-methylimidazolium chloride (C_4Cl) were obtained from Prof. Schrekker (Universidade Federal do Rio Grande do Sul, Porto Alegre-RS, Brazil).[42]

All chemicals were used without any further purification.

2.2 Synthetic procedures

Networks. The epoxy networks were prepared by the reaction of DGEBA with di- and monoamines at a total stoichiometric ratio of functional groups (C_{epoxy}:C_{NH} = 1:1). Content of monoamines in the networks is characterized by molar fraction of aminogroups *x* in the amine mixture belonging to monoamines; $x = [NH_2]_{mono} / ([NH_2]_{mono} + [NH_2]_{di})$ (see Scheme 1B).

Nanocomposites. The two step synthesis was applied.[38] (i) 2 wt. % of BF_3MEA with respect to TMOS was mixed with the epoxy resin for 30 min at 70 °C. After that, an optional content of TMOS was added to the DGEBA-BF_3MEA mixture and speedily mixed for another 30 min. Then 0.2 wt. % of ionic liquid was added (if mentioned in a sample code) to the mixture and mixed for 30 min more. (ii) Stoichiometric equivalent weight of diamine was added to the prereacted mixture of TMOS in the epoxy resin and mixed for 30 min. In the case of bimodal networks Laromin, ATBN together with EDA were added to the epoxy resin and stirred for 20 min. The following curing regime was applied: 90 °C for 2 h; 130 °C for 16 h and the postcuring under vacuum for 5 h at 190 °C or 210 °C in the case of Laromin containing networks.

The content of silica in nanocomposites was indicated according to the weight fraction of TMOS with respect to DGEBA used at the nanocomposite synthesis. The amount of TMOS indicated as T7, 14, 25 and 40 corresponds to the 2.6, 5.4, 9.6 and 15.2 wt. % of nanosilica, respectively.

The studied systems were designated according to the diamine of the network: D230, D400, ATBN (A), EDA (E), Laromin (L), presence of monoamine MY(molar fraction *x*), content of silica T(7-40) and presence of IL (abbreviation). For example DGEBA-D230-M600(0.05)-T(14)-C_4Cl or bimodal network DGEBA-A(0.3)-E(0.2)-L(0.5)-T(7)-$C_{10}BF_4$.

Dual SM nanocomposite. Two different amines D230 and D400 were used to prepare the dual SM nanocomposite according to the procedure discussed above. Both nanocomposite mixtures were placed on the Teflon wafer separated by a thin silicone bar. During the reaction at a high enough viscosity the silicone bar was removed and two halves of the specimen were mingled at the interphase.

2.3. Methods

The mechanical tests were performed by using the ARES G2 apparatus (TA Instruments).

Dynamic Mechanical Thermal Analysis. The temperature dependence of the complex shear modulus of rectangular samples was measured by oscillatory shear deformation at the constant frequency of 1 Hz and at the heating rate of 3 °C min^{-1}. Glass transition temperature T_g was evaluated as a maximum of the loss factor tan δ. The rubbery modulus was determined at temperature $T=T_g+30$ °C.

Tensile test experiments were performed at axial force with the constant linear speed of 0.06 mm min^{-1} (unless stated otherwise) at T_d = 100 °C or at T_d = 120 °C in the case of bimodal networks. Five rectangular specimens with dimensions 25 x 5 x 1 mm were tested for each sample. The toughness was evaluated as an area under the stress-strain curve.

Stress relaxation was measured by transient stress relaxation mode at a strain λ = 1.07 at T_d = 100 °C.

2.4. Shape-Memory properties

SM behaviour was followed in the temperature region T = 25 - 100 °C, with the setting temperature T_S = 25 °C, transition temperature $T_{trans} = T_g$ and deformation temperature T_d = 100 °C or T_d = 120 °C in the case of bimodal networks. The following parameters were determined to evaluate the shape-memory behaviour: shape fixity, recovery stress (at constrained mode) or recovery rate and extent of recovery (at unconstrained mode).

Shape fixity was measured both in stretching (linear) and in bending mode. The sample was heated and deformed to the

length l_d or to the angle Θ_d = 90° at the deformation temperature. Subsequently, the deformed sample was quickly cooled to the setting temperature and kept at T_S = 25 °C for 6 month. The change of the and the angle in time was recorded. Shape fixity was evaluated as $R_f = 1 - [(l_d - l_f)/l_d] \times 100\%$, where l_d and l_f are the length in the deformed state at deformation temperature and in the frozen state after 6 months, respectively. The bending mode was applied as well because of easy visualization of shape fixity.

Shape recovery triggered by heating up to T_d was evaluated in the linear mode as $R_r = [1 - (l_r - l_0)/l_0] \times 100\%$, where l_0 – initial non-deformed length, l_r - recovered length.

Rate of shape recovery was evaluated in the bending mode by following the angle change of the deformed specimen in time.

Constrained recovery – recovery stress (σ_r).

The recovery stress σ_r was measured on ARES G2 equipped with a thermal chamber and liquid nitrogen tank. The rectangular sample 25 x 5 x 1 mm was heated up to deformation temperature T_d and extended up to 60% of the previously determined strain at break, $\lambda_d = 0.6\lambda_b$, at a rate of 0.06 mm min^{-1}, unless stated otherwise. In all experiments $\lambda_d >$ 1.07, which corresponds to the thermoelastic inversion point of epoxy systems.[13,43] The sample was subsequently cooled at a rate of 10 °C min^{-1} (unless stated otherwise) down to the setting temperature T_S while maintaining the load and kept for 10 minutes to completely freeze and store the stress within the sample. Only then the sample was unloaded. For the constrained recovery the sample was fixed, the length was kept constant and heated up to deformation temperature. The recovery stress triggered by heating was recorded.

3. Results and discussion

The epoxy-silica nanocomposites have been designed as promising high performance SMP applicable in the temperature range between T_{room} and T = 100 °C.

3.1. Synthesis of SM networks and nanocomposites.

The nanocomposites based on epoxy-amine networks were prepared and the following structural parameters or synthesis conditions were varied in order to modify the nanocomposite structure and morphology: (i) crosslinking density of the epoxy network,, (ii) presence of long pendant chains in the network, (iii) content of nanosilica, (iv) presence of IL at the synthesis.

Epoxy networks. Three types of the networks were synthesized. (i) The networks of different crosslinking density were prepared by crosslinking of DGEBA with diamines of different length, including poly(oxypropylene) diamines, Jeffamines D230 (M = 230) and D400 (M = 430) (see Scheme 1A), and amino-terminated butadiene-acrylonitrile copolymer, ATBN (M = 3600). (ii) The networks containing long pendant chains were prepared by partial substitution of diamines with monoamines, polyetheramines, Jeffamine M600 (M ~ 600) and M1000 (M ~ 1000) (Scheme 1B). (iii) The bimodal networks with the bimodal distribution of crosslinking density were prepared by crosslinking of DGEBA with two diamines of different length, ATBN (M = 3600) and 4,4'-methylenebis(2-methylcyclohexylamine) (Laromin) (M = 238) (Scheme 2). The network involves long flexible sequences of ATBN (R3 sequence) and rigid sequences of Laromin (R4) as well as compatibilizing parts of EDA (R5).

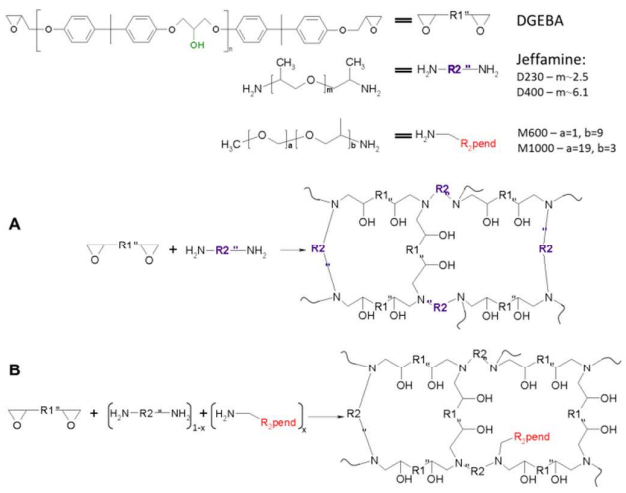

Scheme 1 Structure of the (A) networks DGEBA-D230 and DGEBA-D400, (B) networks with pendant chains DGEBA-D230-M

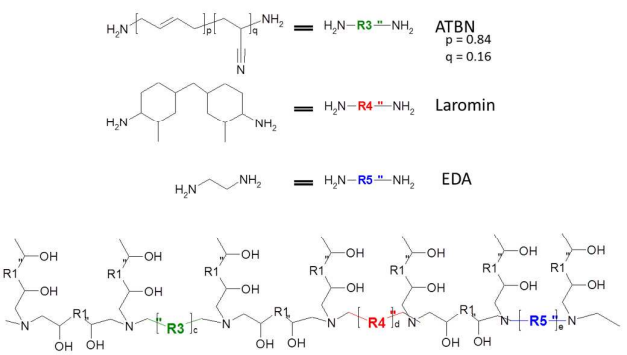

Scheme 2 Structure of the bimodal network

Epoxy-silica nanocomposites. The nanocomposites were prepared by *in situ* generation of nanosilica within the epoxy-amine matrix by the non-aqueous sol-gel process (Scheme 3 B). The non-hydrolytic polycondensation was initiated by proteolysis of TMOS using BF_3MEA (Scheme 3A).[38,39] During the nanocomposite formation the interphase epoxy-silica covalent grafting occurs [38] (Scheme 3C). The sequential synthesis was applied (see Experimental).

The imidazolium based ILs were used at synthesis of the epoxy-silica nanocomposites serving as multifunctional agents at the sol-gel process. The IL acts as a catalyst, surfactant and an efficient agent controlling the silica structure as well as the nanocomposite morphology by forming strong physical interphase interactions, silica-IL-epoxy matrix.[41]

The non-aqueous sol-gel procedure and application of ILs make it possible to control the interphase interaction, both covalent and physical, (see Scheme 4) and fine tuning the

structure and morphology of the nanocomposites as well as to enhance their mechanical properties.[38-41]

The applied synthesis leads to formation of well homogeneous epoxy-silica nanocomposites. The TEM micrographs in Fig. 1 show a comparison of morphology of the nanocomposites prepared by the classical aqueous sol-gel process, by the non-aqueous procedure and that prepared in the presence of the IL. While the reference "aqueous nanocomposite" exhibits non-uniform dense particles forming aggregates with a broad size distribution, the non-aqueous sol-gel process results in a finer morphology of loosely packed aggregates and the IL promotes formation of morphology composed of uniformly dispersed particles without larger aggregates.

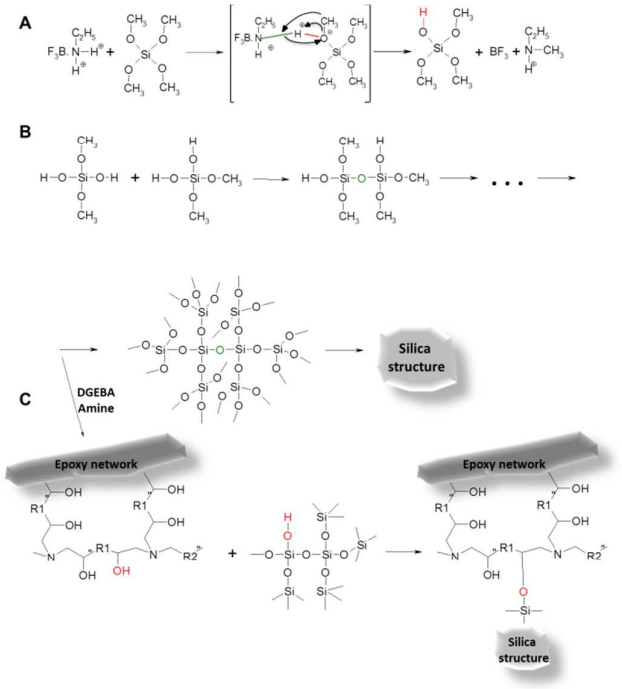

Scheme 3 Formation of epoxy-silica nanocomposites: (A) Proteolysis of TMOS, (B) Silica formation, (C) Build-up of the nanocomposite, covalent bonding between epoxy network and silica domain

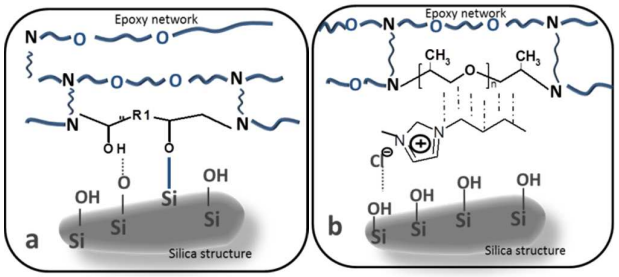

Scheme 4 Representation of the corresponding nanocomposite interphase interactions: (a) covalent grafting epoxy-silica (b) physical interactions in presence of IL.

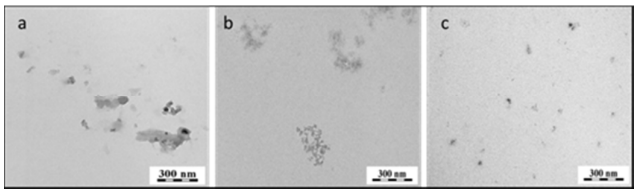

Fig.1 TEM micrographs of the nanocomposite DGEBA-D400-T(14) prepared by (a) aqueous sol-gel process, (b) non-aqueous sol-gel process, (c) non-aqueous procedure in the presence of the IL C_4Cl.

3.2. High performance SMP – design of structure

SMPs undergo a shape recovery triggered by heating above the transition temperature (unconstrained recovery). In the case of the fixed strain (constrained recovery) the material shows a recovery of the stress. This recoverable stress depends on the mechanical stress at the initial deformation at rubbery state, which is internally stored into the polymer upon the cooling/fixing process. Under ideal conditions and no losses, at a perfect shape fixity and no stress relaxation it holds according to the theory of rubber elasticity

$$\sigma_r \sim \sigma_d = G_r(\lambda_d - \lambda_d^{-2}) \qquad (1)$$

where σ_r is the recovery stress, G_r and σ_d are modulus and stress under deformation at rubbery state, respectively, λ ($=l/l_0$) is the deformation ratio, l and l_0 are the deformed and initial length of the sample, respectively. The stress at recovery thus depends on rubbery modulus and deformation λ. Gall et al. observed that, the recovery stress directly scales with the rubbery modulus and the network stress at the initial deformation.[44] Hence, the design of the polymer with a high rubbery modulus allowing a high deformation at rubbery state is a way to synthesis of the high performance SMP.

Moreover, the investigation is focused on the systems showing shape memory properties in the temperature region $T = T_{room}$ – 100 °C (or 120 °C), where T_{room} is the setting temperature T_s. Consequently, adjustment of T_g is necessary as well.

3.2.1 Control of the thermomechanical properties

Crosslinking density and chain flexibility.

The thermomechanical properties of a perspective SMP are tuned in such a way to reach a high rubbery modulus while to keep T_g in the application window of a polymer.

Rubbery modulus of elasticity of polymer networks is determined mainly by crosslinking density ν:

$$G_e = \nu RTA + \text{physical contribution} \qquad (2)$$

G_e is equilibrium shear modulus at rubbery state, A is front factor (A = 1 for affine networks, A = (f-2)/f for phantom networks, f is functionality of a crosslinker).

Physical contribution to a modulus involves physical crosslinking by trapped chain entanglements or by formation of self-assembly domains acting as network junction. The crucial contribution, however, is given by presence of fillers in composites or nanocomposites. Hydrodynamic effect of filler resulting in strain amplification, formation of a rigid interphase

layer due to an interphase interaction polymer-filler giving rise to an increasing efficient fraction of a filler, physical crosslinking through filler domains or filler network build-up at percolation of filler structure are the reasons of a polymer reinforcement by filler.

The increase in crosslinking density of a network to enhance modulus gives rise to increase in T_g as well. Therefore, there are certain limits of crosslinking density in order to keep T_g in the application window of a SMP. In addition to crosslinking density also the chain stiffness or flexibility affects the modulus by modifying front factor A in Eq.2.[45] Stiff chains in a network lead to a higher modulus and higher T_g with respect to the network containing flexible chains.[20] Due to the simultaneous effect of a network structure on both modulus and T_g a careful tuning of a polymer structure is necessary in order to optimize the thermomechanical properties for a SMP application.

We have studied the epoxy-amine networks of various crosslinking density and flexibility of network chains. They were prepared by using four amine crosslinkers: Jeffamines D230 and D400, Laromin and ATBN. Generally, it holds for crosslinking density $\nu \sim 1/M_C$, where M_C is molecular weight of the elastically active chain between crosslinks, that can be controlled, e.g., by a structure of a crosslinker. The molecular weights of the applied amines are as follows: M(D230) = 230, M(D400) = 430, M(Laromin) = 238, M(ATBN) = 3600. Fig.2 shows the effect of length of the amines on modulus in rubbery state G' and T_g of the epoxy networks. The modulus increases in the series DGEBA-ATBN < DGEBA-D400 < DGEBA-D230 in accordance with increasing crosslinking density. The higher modulus of DGEBA-Laromin network compared to DGEBA-D230, possessing approximately the same crosslinking density, is a result of a higher rigidity of the cycloaliphatic amine with respect to polyether network chains. The modulus of these networks enhances from 1.5 MPa up to 20 MPa. However, only the networks DGEBA-D400 and DGEBA-D230 display T_g in the suitable application window, at T_g = 50 °C and T_g = 91 °C, respectively.

Physical crosslinking.

Introducing the physical crosslinks in a covalent network is another approach to increase modulus. We have studied the epoxy networks DGEBA-D230 containing long pendant polyoxypropylene chains (see Scheme 1 B). The incorporation of monoamines M600 and M1000 in the network results in lowering of the total amine functionality and in decrease in chemical crosslinking density. The rubbery modulus, however, on the contrary increases at a small amount of the monoamines as shown in Fig.3. This is a result of physical crosslinking due to self-assembling or formation of entanglements between dangling chains. At a small fraction of the monoamines, x = 0.05, this effect dominates and the rubbery modulus enhances with respect to the unmodified DGEBA-D230 network. In contrast, the flexible pendant chains give rise to decrease in T_g of the network. Consequently, the thermomechanical properties of these networks can be tuned by controlling chemical and physical crosslinking in such a way that modulus increases and T_g simultaneously diminishes. This approach is beneficial for our SMP by enhancing rubbery modulus while keeping T_g in the application window. In the case of the network DGEBA-D230-M1000 (x = 0.05) the modulus grows from 10 MPa of the unmodified network to 14 MPa and T_g decreases from 91 °C to 73 °C.

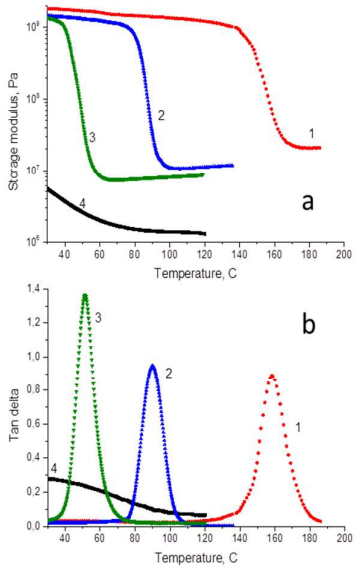

Fig.2 Storage modulus (a) and loss factor tan δ (b) of epoxy networks as functions of temperature: 1 DGEBA-Laromin, 2 DGEBA-D230, 3 DGEBA-D400, 4 DGEBA-ATBN.

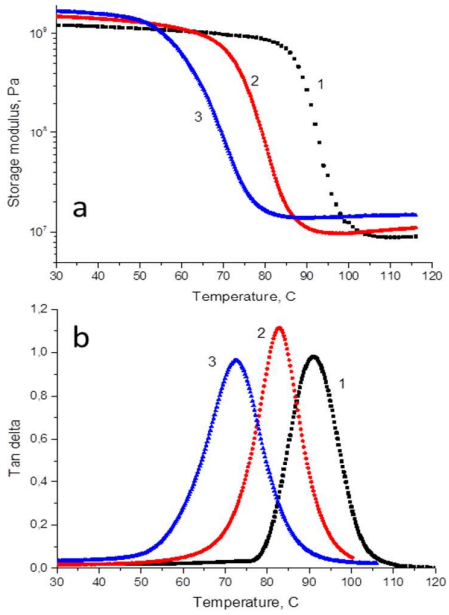

Fig.3 Storage modulus (a) and loss factor tan δ (b) of the DGEBA-D230 with pendant chains as functions of temperature: 1 DGEBA-D230, 2 DGEBA-D230-M600 (x = 0.05), 3 DGEBA-D230-M1000 (x = 0.05).

Nanofiller effect.

The most pronounced reinforcement of the epoxy networks was achieved by incorporation of silica nanofiller. Thermomechanical behaviour of the nanocomposites DGEBA-D400-nanosilica is illustrated in Fig. 4. The rubbery modulus is significantly enhanced in the nanocomposites by 100 - 200% with respect to the neat DGEBA-D400. The hybrid network containing 9.6 wt. % silica (T25) displays the modulus G_r = 20 MPa. At the same time T_g of the nanocomposites is raised due to immobilization of the network chains by interaction with silica domains and formation of a rigid interphase layer (see Scheme 4a). In the case of the nanocomposite DGEBA-D400-T(25) the glass transition temperature is increased by 15 °C. This T_g rise limits the application of silica reinforcement to the DGEBA-D400 matrix only because the DGEBA-D230 based nanocomposite does not fit in the application temperature window due to too high T_g. The high content of silica is moreover manifested by broadening of glass transition. This is a result of a system inhomogeneity. The nanocomposite shows a wide distribution of chains' dynamics in the vicinity of the silica domain ranging from severely immobilized chain sequences to less restricted chains sterically far from nanofiller. In addition, incompletely reacted siloxane/silica domains contribute to the broadness of the transition.[39] The wide transition limits application of nanocomposites as a SMP. It gives rise to a slower recovery at heating and in the low temperature region the broad transition decreases the modulus at setting temperature G_S which is responsible for the shape fixity. G_s is lowered by 20-30 %, however, it is still high enough to provide the excellent shape fixity. Optimization of the silica content is thus necessary in order to avoid too high T_g and excessive widening of the glass transition.

Ionic liquids' effect.

The IL increases both rubbery modulus and T_g of the nanocomposite. Figure 4 shows that this effect is more pronounced at a higher silica content (cf. curves 2 and 5 for T14, curves 3 and 6 for T25, curves 4 and 7 for T40). Crucial, however, is the effect of the IL on morphology and homogenization of the nanocomposite as revealed in Fig.1. The enhanced homogeneity due to an interphase interaction (see Scheme 4b) is reflected in thermomechanical properties. Figure 4 displays a narrowing of glass transition of the nanocomposite promoted by the IL (cf. curves 5 and 2). The sharp transition results in a faster quenching and in a better shape fixity. This is, however, true only at a low and medium silica amount. The optimum nanocomposite thermomechanical properties were accomplished by using 5 - 10 wt. % silica (the hybrids T (14)-(25)). At a higher TMOS content (T40), the T_g is too high and homogenization does not work; glass transition is too broad (curve 7). Three types of ILs were used in synthesis of nanocomposites; C_4Cl, C_4BF_4 and $C_{10}BF_4$. However, no difference in their effect on morphology and thermomechanical properties was observed.

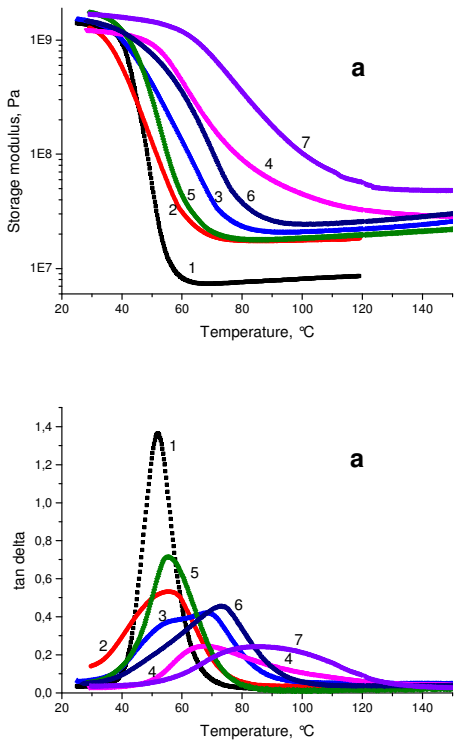

Fig.4 Storage modulus (a) and loss factor tan δ (b) of the DGEBA-D400 based hybrids as functions of temperature: 1 DGEBA-D400, 2 DGEBA-D400-T(14), 3 DGEBA-D400-T(25), 4 DGEBA-D400-T(40), 5 DGEBA-D400-T(14)-C_4Cl, 6 DGEBA-D400-T(25)-C_4Cl, 7 DGEBA-D400-T(40)-C_4Cl.

The most suitable thermomechanical properties of the SMP were achieved by combination of the above discussed effects of the physical crosslinking by pendant chains and the reinforcement with nanosilica generated under IL assisted catalysis (see Fig. 5). Because of the T_g lowering by plasticizing pendant chains also the higher-T_g network DGEBA-D230 could be used as a matrix for the epoxy-silica nanocomposite. The T_g of the corresponding DGEBA-D230-monoamine-nanosilica-IL system is kept in the application window. This complex nanocomposite profits as SMP from the following thermomechanical properties; (i) high modulus due to silica reinforcement and physical crosslinking, (ii) T_g in the application window due to plasticizing effect of flexible pendant chains, (iii) narrow glass transition because of nanocomposite homogenization by action of ILs.

The thermomechanical properties of the studied SM polymers are characterized in Table S1 (in Supporting informations.)

3.2.2 Tensile stress-strain behaviour

The proper thermomechanical properties of a material, including T_g, broadness of the transition, rubbery and setting moduli G_r, G_s, are prerequisite for an optimum shape memory behaviour. In addition, however, the structure design must take into account the material behaviour at deformation which is closely related to the shape memory process.

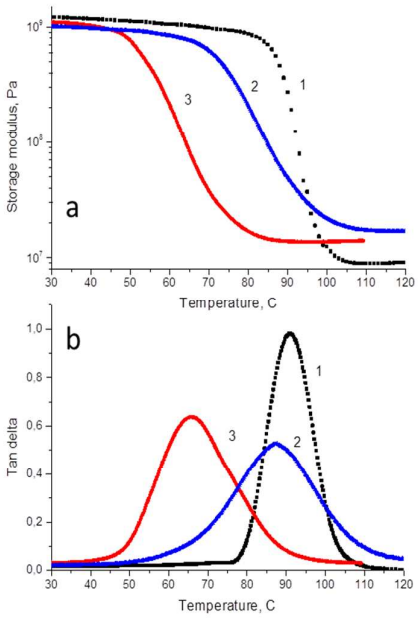

Fig.5 Storage modulus (a) and loss factor tan δ (b) of the DGEBA-D230-T(7) with pendant chains: 1 DGEBA-D230, 2 DGEBA-D230-M600(0.05)-T(7), 3 DGEBA-D230-M1000(0.05)-T(7).

We have investigated the tensile stress-strain properties of the examined systems at deformation temperature in rubbery state at T_d = 100 °C or 120 °C. The results of DGEBA-D400 based network and nanocomposites are displayed in Fig.6. The polyether Jeffamine based epoxy networks DGEBA-D400 and DGEBA-D230 are considered to belong among the toughest epoxy thermosets. The DGEBA-D400 network (curve 1) shows an elongation at break ε_b = 20% in rubbery state and tensile strength σ_b = 2.3 MPa. The Figure 6 reveals that the epoxy network modification leads to a dramatic improvement of tensile properties. Incorporation of nanosilica in the network (curve 2) brings about a significant enhancement of modulus and strength, while only a slight reduction of deformability (ε_b). Another improvement is achieved by application of the IL at synthesis of nanocomposites (curves 3 and 4). The beneficial effect of the IL is manifested by a pronounced increase in toughness of the nanocomposites; both extensibility and tensile strength are enhanced. This is a result of modification of epoxy-silica interphase by IL (see Scheme 4b). The strong physical dynamic interphase interaction undergoes a breaking-formation process under stress which is responsible for the enhanced toughness. The material toughness corresponds to the mechanical energy absorbed by a material before break and generally it is characterized by area under the stress-strain curve. The polymer toughness was found to be the decisive materials property governing a shape memory behaviour as discussed below. The similar, but less pronounced trend in tensile behaviour, was observed also at room temperature as shown in Table S2 (in Supporting informations

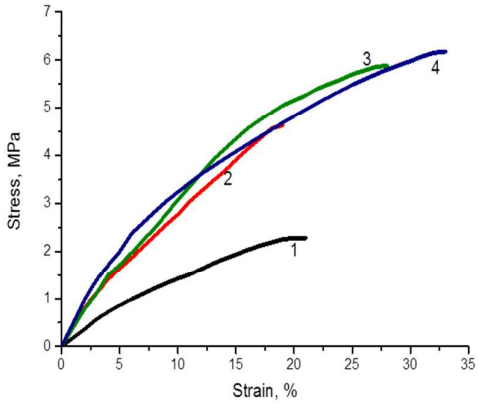

Fig.6 Stress–strain behaviour of the SM network and nanocomposites at T_d: 1 DGEBA-D400, 2 DGEBA-D400-T(14), 3 DGEBA-D400-T(14)-C_4Cl, 4 DGEBA-D400-T(25)-C_4Cl.

.

Highly deformable SM epoxy polymers – bimodal networks. The extensibility, i.e. strain at break λ_b, of a polymer network based material is related to the crosslinking density and generally it is expressed as $\lambda_b \sim M_c^{1/2}$. The polymer deformability thus could be increased at the expense of modulus only, as $G \sim 1/M_c$.

The high-molecular weight amine crosslinker ATBN (M = 3600) allows to prepare the highly extensible epoxy network. Figure 7 illustrates the corresponding stress-strain curve at T_d = 120 °C revealing the high elongation at break ε_b = 280% (curve 2). The DGEBA-ATBN elastomer is rubbery at room temperature and hence the combination with the high-T_g, but less ductile, DGEBA-Laromin network (Fig.7 curve 1 and Fig.8 curve 1) was applied in order to increase T_g of the corresponding bimodal network. The bimodal network (see Scheme 2) of the molar composition, DGEBA-ATBN(n=0.3)-Laromin(n=0.7), exhibits still a high extensibility; ε_b = 100 % (Fig.7, curve 3) and T_g occurs in the application window, T_g = 85 °C (see Fig.8 curve 2).

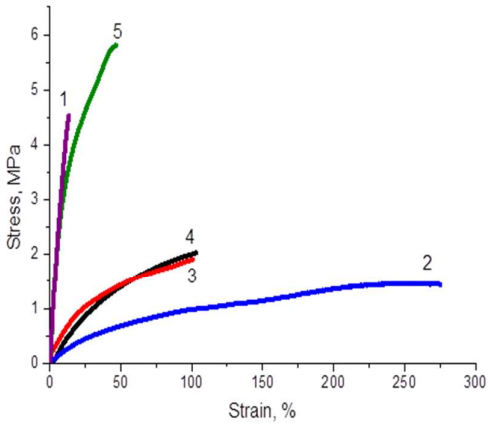

Fig.7 Stress–strain behaviour of the of the SM nanocomposites at T_d: 1 DGEBA-Laromin, 2 DGEBA-ATBN, 3 DGEBA-A(0.3)-L(0.7), 4 DGEBA-A(0.3)-E(0.2)-L(0.5), 5 DGEBA-A(0.3)-E(0. 2)-L(0.5)-T(14)

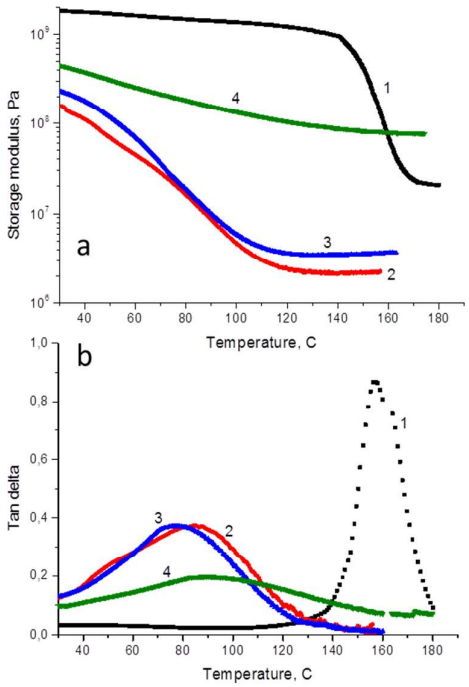

Fig.8 Storage modulus (a) and loss factor tan δ (b) of the bimodal systems: 1 DGEBA-Laromin, 2 DGEBA-A(0.3)-L(0.7), 3 DGEBA-E(0.2)-A(0.3)-L(0.5), 4 DGEBA-A(0.3)-E(0.2)-L(0.5)-T(14).

This system is phase separated, containing the mixed phase of partially miscible epoxy and rubbery components with a broad glass transition (T_g = 85 °C), and a dispersed rubbery phase (T_g= -45 °C, not shown in Fig.8). The low temperature shoulder in addition to maximum in the tan δ curve in Fig.8b, however, reveals a partial phase separation and incompatibility of the two networks even within the „miscible phase“. Because of a high fraction of the separated ATBN phase the modulus at room temperature is relatively low, G_s = 160 MPa, which results in a low shape fixity of the SMP. Improvement of compatibility was achieved by addition of a small amount of crosslinker ethylene diamine (EDA). The corresponding network DGEBA-A(0.3)-E(0.2)-L(0.5) shows a better compatibility as it is obvious from one loss factor peak in Fig.8 (curve 3). The fraction of the dispersed rubbery phase was diminished, however, not eliminated. This modification leads to a slight reduction of *Tg* and narrowing of glass transition as well as to increase both in G_r and G_s. However, G_s is still low (= 240 MPa) and the tensile properties are not significantly changed, ε_b = 103 % (Fig.7, curve 4). The substantial improvement of mechanical properties was achieved by using nanofiller. The nanocomposite containing 5 wt. % silica (T14) (Fig.7, curve 5) displays enhancement of strength by 200 % and G_r by more than an order of the magnitude up to 76 MPa. The extensibility is relatively high, ε_b = 47% and G_s increases. Even this nanocomposite involves a small fraction of the dispersed rubbery phase.

The bimodal network based nanocomposite is a very tough material. The following series displays the studied systems with increasing toughness as evaluated from area under the stress-strain curve: DGEBA-D230 < DGEBA-D230-M-T < DGEBA-D400 < DGEBA-D400-T < DGEBA-D400-T-IL < DGEBA-A(0.3)-L(0.7) < DGEBA-A(0.3)-E(0.2)-L(0.5) < DGEBA-A(0.3)-E(0.2)-L(0.5)-T. The results thus unveil that toughness enhances by (i) increasing molecular weight of the amine crosslinker, (ii) incorporation of silica nanofiller, (iii) application of IL in synthesis of nanocomposites, (iv) formation of bimodal networks. Based on this finding one can design structure of a system in order to tune the toughness of a material.

3.2.3 Shape memory properties

The following SM characteristics were evaluated: shape fixity, shape recovery, rate of recovery and recovery stress.

Recovery stress. The comparison of thermomechanical, tensile and shape memory results demonstrates that the generally accepted prediction $\sigma_r \sim G_r$ is not well satisfied. For instance, the nanocomposites DGEBA-D400-T(14) and DGEBA-D400-T(14)-C_4Cl show the same rubbery modulus G_r, however the nanocomposite prepared in presence of IL exhibits 4 times higher recovery stress. The results reveal that a recovery stress of a SMP is determined mainly by the material toughness. Figure 9 illustrates the experimentally determined σ_r of the studied systems as a function of their toughness. The toughest nanocomposites based on bimodal networks and those prepared by using IL exhibit the highest recovery stress. Particularly, the highest value was achieved in the bimodal nanocomposite network DGEBA-A(0.3)-E(0.2)-L(0.5)-T(14) showing σ_r = 3.7 MPa. Moreover, in contrast to an irregular scatter of experimental data in the case of the dependence σ_r vs G_r, the plot σ_r vs toughness in Fig. 9 displays an unambiguous universal trend involving all investigated systems. The structural effect on recovery stress exhibits the similar trend as for toughness. The recovery stress increases in the systems filled with silica and particularly in the nanocomposites prepared by using ILs. A slight enhancement was observed after incorporation of a small amount of pendant chains. Mainly, however, the recovery stress is

enhanced in the nanocomposites based on bimodal networks. These structural effects in SM polymers on recovery stress are shown in Table S1 (in Supporting information). One has to take into account, however, that the comparison of the effect in different systems could be slightly distorted by the fact that the measurement was performed at the constant temperature T_d for all systems, excluding bimodal networks, disregarding T_g and the temperature difference ΔT (=T_d-T_g) in the particular system.

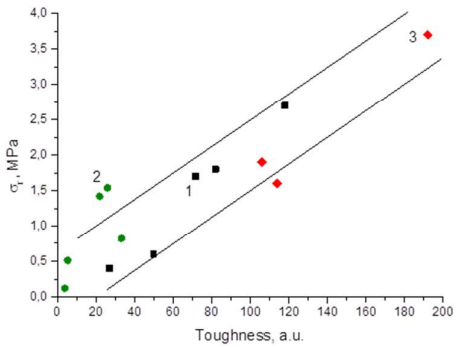

Fig.9 The recovery stress in SMPs as a function of their toughness for: 1 – DGEBA-D400 and 2 – DGEBA-D230 based systems, 3 – DGEBA-ATBN-Laromin based bimodal systems.

The limit of an achievable recovery stress is given by the stress at λ_d (= 0.6 λ_b, see Experimental) at deformation temperature (T_d). This is an ideal potential, however the real recovery stress is determined by the energy loss during the shape memory cycle. The efficiency to store the elastic energy and memorize the initial state during the cooling / heating processes is characterized approximately by the ratio σ_r/σ_d (~ σ_r/σ_b). According to this criterion, the shape memory efficiency is reduced in the nanosilica filled system, however it is improved by application of the IL at synthesis of nanocomposites.

The other SM properties correspond to typical epoxy systems exhibiting the excellent shape fixity and recovery as displayed in Tab.1.

Shape fixity. All systems exhibit 100 % shape fixity after 6 months with the exception of the bimodal networks containing ATBN. R_f depends on modulus at setting temperature G_s. Decrease in shape fixity occurs in polymers showing G_s < 500 MPa, which is the case of the bimodal networks (see Table S1). The reduced fixity, R_f = 86 %, was determined in the DGEBA-A(0.3)-E(0.2)-L(0.5) bimodal network displaying a low modulus, G_s = 240 MPa, as well as in the corresponding nanocomposite involving 5 wt. % of nanosilica (T14), R_f = 95 %, G_s = 450 MPa.

Shape recovery. The SMPs show almost complete shape (linear) recovery under nonconstrained conditions. A small reduction of shape recovery due to an irreversible deformation was observed in the systems with strong physical interactions and inhomogeneities. This is the case of the nanocomposites with a high nanosilica amount mainly in the bimodal networks and the networks with long pendant chains undergoing a disentanglement. The IL homogenizes the nanocomposite and prevents thereby this shape recovery reduction which results in perfect recovery, 99.7%.

Rate of recovery. The shape recovery is completed in 15 - 30 s. The slight slowing down within this range was observed in the silica containing nanocomposites in agreement with the general knowledge about a lower recovery speed in the less homogeneous systems.

Table 1 Shape fixity R_f and recovery R_r of epoxy SMPs

SMP system	R_f, %	R_r, %
DGEBA-D400	100	99.95
DGEBA-D400-T(14)	100	99.5
DGEBA-D400-T(40)	100	98.2
DGEBA-D400-T(14)-C_4BF_4	100	99.7
DGEBA-D230-M600(0.1)	100	98.9
DGEBA-D230-M1000(0.1)	100	98.7
DGEBA-A(0.3)-E(0.2)-L(0.5)	86	99.9
DGEBA-A(0.3)-E(0.2)-L(0.5)-T(14)	95	97.9

3.2.4. Viscoelasticity effect

The loss of the stored energy during the SM cycle consists in an irreversible plastic deformation as well as in viscoelastic properties and time dependent behaviour of polymers. It is reflected by a reduced shape fixity, incomplete shape recovery and a lower recovery stress, $\sigma_r < \sigma_d$. Therefore, a viscoelasticity effect and a stress relaxation are to be taken into account in order to better understand the SM efficiency of polymers. The stress at deformation of a viscoelastic polymer includes the elastic, equilibrium part and the viscoelastic one,

$$\sigma(t) = \sigma_e + \sigma_0 \exp(-t/\tau)^m \qquad (3)$$

where σ_0 and σ_e are initial (at t = 0) and equilibrium stress at deformation, respectively, τ is relaxation time.

The stress relaxation in the studied systems at the deformation temperature T_d is displayed in Fig.10. The almost "ideal elastic" network DGEBA-D230 shows a very small viscoelastic effect. Due to a high chemical crosslinking density the stress relaxes quickly and levels off at equilibrium value σ_e in 15 s (curve 1). The behaviour of structurally heterogeneous bimodal network of a lower crosslinking density involves more viscoelasticity, however relaxation is fast (curve 3). Mainly the nanocomposites containing silica nanofiller exhibit a significant viscoelastic effect (curve 2 and 4) because of strong physical interactions and phase inhomogeneity. It is manifested by a pronounced and a relatively slow stress relaxation reaching the equilibrium value in t > 10 min. This is in agreement with literature data reporting an increased relaxation time with the incorporation of nanoparticles.[46]

The viscoelastic behaviour and relaxation of the studied systems is characterized in Tab. 2, where the viscoelasticity effect is expressed, for the sake of simplicity, as $\Delta\sigma_{VE} = (\sigma_0 - \sigma_e) / \sigma_0$. The following structural trends were determined as to the viscoelasticity: (i) increasing crosslinking density of a network leads to a higher elasticity and a faster relaxation, (ii) incorporation of dangling chains enhances viscoelasticity contribution and slows down the relaxation due to physical interactions: slow disentanglement, (iii) presence of nanofiller results in a strong viscoelasticity effect and a slow relaxation, (iv) application of ILs reduces the viscoelasticity and

accelerates relaxation because of improvement of nanocomposites homogeneity.

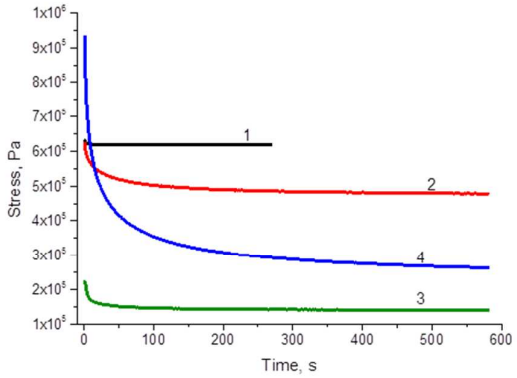

Fig.10 Stress relaxation at T_d: 1 DGEBA-D230, 2 DGEBA-D230-T(14), 3 DGEBA-A(0.3)-E(0.2)-L(0.5), 4 DGEBA-A(0.3)-E(0.2)-L(0.5)-T(14).

Table 2 Relaxation of SMPs at T_d = 100 °C

System	$\Delta\sigma_{VE}$	t_{relax}, min
DGEBA-D230	0.02	0.25
DGEBA-D230-M600(0.1)	0.12	2
DGEBA-D230-T(14)	0.30	>15
DGEBA-D400	0.18	7
DGEBA-D400-T(14)	0.23	>10
DGEBA-D400-T(14)-$C_{10}BF_4$	0.15	9
DGEBA-A(0.3)-E(0.2)-L(0.5)	0.59	5
DGEBA-A(0.3)-E(0.2)-L(0.5)-T(14)	0.75	>10

$\Delta\sigma_{VE}$ - viscoelasticity effect, t_{relax} – time of relaxation up to equilibrium of stress

The strong viscoelastic behaviour could be a reason of the reduced SM efficiency of the nanocomposites. The results reveal that the IL reduces the viscoelastic effect and at the same time improves the SM efficiency corroborating thereby the above hypothesis. These findings unveil the correlation between a morphological homogeneity, viscoelastic behaviour and shape memory efficiency. Minimizing the stress relaxation thus could be another way how to improve the SM efficiency and to reduce the loss of the stored energy.

Consequently, the effects of the nanocomposites structure and synthesis parameters are as follows: (i) silica nanofiller increases G_r, strength and toughness, however SM efficiency is reduced due to a broadening of glass transition and a strong viscoelasticity effect, (ii) the IL used at a synthesis improves homogeneity of a nanocomposite morphology, thereby reducing broadness of the glass transition and viscoelasticity effect and accelerates relaxation; in addition it enhances toughness due to the strong interphase interaction and improves SM performance, (iii) bimodal networks display a high toughness and deformability, being thus promising systems for high performance SMPs, (iv) physical crosslinking by long pendant chains increases Gr without an enhancement of T_g.

3.3 Optimization of the experimental SM procedure

In addition to material structural characteristics also the experimental conditions of the SM procedure can affect the SM performance. The technical conditions include rate and extent of deformation, temperature at deformation, rate of cooling/heating processes, geometry (size) of a sample, etc. We have studied the effect of rate of deformation and rate of cooling. The relative rates of the time dependent processes, such as experimental procedure and polymer relaxation, are crucial. Both slowing down the polymer relaxation and acceleration of experimental procedures prevent or minimize stress relaxation during these steps and enable the quenching the relaxation process before reaching the equilibrium state.
The effect of the deformation and cooling rates on the recovery stress of the nanocomposite DGEBA-D400-T(14)-C_4BF_4 is shown in Table 3. The stress relaxation of this nanocomposite in rubbery state is relatively slow. About 50 % of the nonequilibrium stress is relaxed in 25 s at 100 °C, however the equilibrium is reached only in ~ 9 min. As a result, an effect of the experimental procedure could be expected when freezing the sample within 9 min, while the procedure will significantly affect the SM behaviour in the case of quenching in less than ~ 25 s. The Table illustrates an enhancement of the recovery stress at increasing rates of both deformation and cooling. The effect of rate of deformation was studied at the highest cooling rate in order to eliminate the influence of relaxation at a slow cooling. Similarly, the effect of rate of cooling was followed at the highest deformation rate.

Table 3 Effect of rate of deformation and rate of cooling on recovery stress σ_r of the nanocomposite DGEBA-D400-T(14)-C_4BF_4

Rate of deformation, mm s^{-1}	Rate of cooling, °C min^{-1}	σ_r, MPa	
0.06	10	2.58	reference conditions
0.06	50	2.64	
1	50	2.70	effect of deformation rate
10	50	2.92	
10	10	2.77	effect of cooling rate
10	30	2.78	
10	50	2.92	

The deformation process takes either 1.5 s or up to 5 min according to the rate of deformation in the range 0.06 - 10 mm s^{-1}. At the highest rate the polymer has less time to relax. Thereby, the higher nonequilibrium stress is quenched by cooling, leading thus to the higher stress at recovery. The sample deformation at 100 °C is immediately followed by cooling with a delay 1 - 2 s. According to the rate of cooling it takes about 1 – 8 min for the instrument to cool down the oven from 100 °C to glassy state of the sample and freeze it (in this case T_g = 62 °C). The quick cooling leads to earlier

quenching and increase in σ_r. By applying the highest rates, the recovery stress is enhanced by 15 % with respect to the reference conditions used in all experiments. Under the optimized conditions the recovery stress σ_r = 3.9 MPa was determined in the case of the bimodal network based nanocomposite DGEBA-A(0.3)-E(0.2)-L(0.5)-T(14). The effect of cooling rate is dependent on heat transfer, thermal conductivity of a material and geometry of a sample.

3.4. Dual SM material

The acquired knowledge was used to prepare the dual SM material, the two parts of which can be controlled at different temperatures. The sample in Fig.11 is composed of two halves of different structures, i.e., containing the networks of different T_g as shown in Fig.12. The left hand part is the material based on DGEBA-D400 network while the right hand one involves the DGEBA-D230 network. The narrow middle interphase is the mixed type due to interdiffusion of the reaction mixtures in both parts. The shape recovery of the two parts is triggered by heating up to T_1 = 60 °C and to T_2 = 110 °C, respectively (cf. Fig.12). The Fig.11 discloses that both temperatures Ts_1 = 25 °C and Ts_2 = 60 °C are applicable as the setting temperatures. However, the storage modulus at 60 °C is low, $G_{s(60C)}$ = 300 MPa, resulting in poor shape fixity of the second right-hand part, being only 82 % after 10 days.

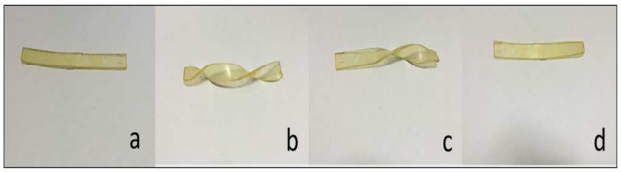

Fig.11 Dual SM effect of the epoxy-silica nanocomposite DGEBA-D230/D400-T(14)-$C_{10}BF_4$: a) initial shape, b) heated up to 110 °C, deformed and cooled down to T_s, c) heating up to 60 °C and d) heating up to 110 °C.

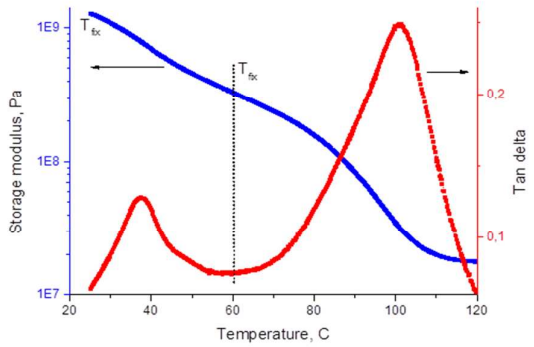

Fig.12 Storage modulus and loss factor tan d of the shape memory nanocomposite with the dual SM effect DGEBA-D230/D400-T(14)-$C_{10}BF_4$ as a function of temperature.

4. Conclusions

The paper deals with the structural design and synthesis of high performance epoxy based SM nanocomposites. They were prepared by *in situ* generation of nanosilica within the epoxy matrix and the special synthesis was employed in order to finely tune their structure. The non-aqueous sol-gel process and application of ILs at synthesis made it possible to control strength of interphase, morphology and mechanical properties of the nanocomposites.

The investigation involved determination of relationships between structure, mechanical properties and the SM properties of the studied polymers. It was found that the recovery stress, as a crucial SM property of high performance systems, is governed by the material toughness, which can be considered as a potential of a material for the SM behaviour at the recovery under constrained conditions. However, a SM efficiency to exploit this potential depends on material morphology and viscoelastic behaviour of the polymer as well as on experimental conditions of the SM procedure. The shape fixity and recovery under nonconstrained conditions were proved to be controlled mainly by the material thermomechanical properties such as moduli at deformation and setting temperatures, G_r, G_s, the T_g and broadness of the glass transition.

Because of these correlations, the structure of SM systems was designed in such a way to enable control of (i) thermomechanical, (ii) tensile mechanical and (iii) viscoelastic properties in order to improve their SM performance. The thermomechanical properties were tuned and T_g of SMPs were adjusted by optimization of crosslinking density of the epoxy matrix and flexibility of polymer chains, by introducing physical crosslinks and silica nanofiller to increase rubbery modulus G_r and by application of the IL at synthesis in order to narrow glass transition. Tensile properties, toughness, were determined to be enhanced by silica nanofiller and by application of the IL. Moreover, the bimodal epoxy networks showed a very high toughness and enabled a high extensibility of the SMP. The effect of polymer viscoelasticity and relaxation, as a property deteriorating the efficiency of SM performance, is reduced by increasing a system elasticity and homogeneity; by enhancing crosslinking density and by application of the IL.

The characterization of nanocomposites as SMPs is as follows. The reinforcement by nanosilica increases G_r and toughness, as well as the recovery stress, however SM efficiency is reduced because of a strong viscoelasticity effect. Beneficial is the influence of the IL strengthening the interphase interaction and improving homogeneity of nanocomposite morphology. As a result, the toughness is increased and viscoelasticity reduced, thereby enhancing the SM performance. Also the concept of bimodal networks is promising. Based on the knowledge of the corresponding relationships the high performance epoxy based SM nanocomposite was synthesized showing the high recovery stress σ_r = 3.9 MPa or high deformability ε_b = 103 %. Moreover, the study contributed to the better understanding of the SM behaviour of polymers.

Acknowledgements

The authors acknowledge the financial support the Grant Agency of the Czech Republic (P108/12/1459). The authors thank to Prof. Schrekker (Universidade Federal do Rio Grande do Sul, Porto Alegre-RS, Brazil) for the ionic liquids. Sergii Ponyrko is thankful to the Charles University in Prague for the financial support.

References

1 N. Rapoport, *Prog. Polym. Sci*., 2007, **32**, 962.
2 H. Y. Jiang, S. Kelch and A. Lendlein, *Adv. Mater*., 2006, **18**, 1471.
3 C. Liu, H. Qin and P. T. Mather. *J. Mater. Chem*., 2007, **17**, 1543.
4 H. Koerner, G. Price, N. A. Pearce, M. Alexander and R. A. Vaia, *Nat. Mater*., 2004, **3**, 115.
5 C. Liu, S. B. Chun, P. T. Mather, L. Zheng, E. H. Haley and E. B. Coughlin, *Macromolecules*, 2002, **35**, 9868.
6 Y. Kagami, J. P. Gong and Y. Osada, *Macromol. Rapid Commun.*, 1996, **17**, 539.
7 K. Sakurai, H. Tanaka, N. Ogawa and T. Takahashi, *J. Macromol. Sci., Phys.*, 1997, **36**, 703.
8 J. Diani, Y. Liu, and K. Gall, *Polym. Eng. Sci*., 2006, **46**, 486.
9 J. M. Jani, M. Leary, A. Subic and M. A. Gibson, *Mater. Des*., 2014, **56**, 1078.
10 K. Kumar and D. C. Lagoudas, Shape memory alloys modelling and engineering applications chapter 1: introduction to shape memory alloys. Springer US, 2008.
11 A. Lendlein and R. Langer, *Science*, 2002, **296**, 1673.
12 I. A. Rousseau, *Polym. Eng. Sci*., 2008, **48**, 2075.
13 I. A. Rousseau and T. Xie, *J. Mater. Chem*., 2010, **20**, 3431.
14 D. M. Feldkamp and I. A. Rousseau, *Macromol. Mater. Eng*., 2010, **295**, 726.
15 X. H. Jing, Y. Y. Liu, Y. X. Liu, Z. G. Liu and H. F. Tan, *J. Appl. Polym. Sci.*, 2014, **131**, 40853.
16 J. S. Leng, X. L. Wu and Y. J. Liu, *Smart Mater. Struct*., 2009, **18**, 095031.
17 M. A. Di Prima, K. Galla, D. L. McDowella, R. Guldbergb, A. Linb, T. Sandersonc, D. Campbelle and S. C. Arzbergere, *Mech. Mater*., 2010, **42**, 405.
18 R. Biju, C. Gouri and C. P. R. Nair*, Eur. Polym. J*., 2012, **48**, 499.
19 X. L. Wu, S. F. Kang, X. J. Xu, F. Xiao and X. L. Ge, *J. Appl. Polym. Sci*., 2014, **131**, 40559.
20 T. Xie and I. A. Rousseau, *Polymer*, 2009, **50**, 1852.
21 C. M. Yakacki, S. Willis, C. Luders and K. Gall, *Adv. Eng. Mater.*, 2008, **10**, 112.
22 A. B. Leonardi, L. A. Fasce, I. A. Zucchi, C. E. Hoppe, E. R. Soule, C. J. Perez and R. J. J. Williams, *Eur. Polym. J*., 2011, **47**, 362.
23 N. Zheng, G. Fang, Z. Cao, Q. Zhao and T. Xie, *Polym. Chem*., 2015, **6**, 3046.
24 J. Cui, K. Kratz, M. Heuchel, B. Hiebl and A. Lendlein, *Polym. Adv. Technol*., 2011, **22**, 180.
25 Y. Bellouard, *Mater. Sci. Eng., A*, 2008, **481**, 582.
26 E. Hornbogen, *Adv. Eng. Mater*., 2006, **8**,101.
27 P. Miaudet, A. Derré, M. Maugey, C. Zakri, P. M. Piccione, R. Inoubli and P. Poulin, *Science*, 2007, **23**, 1294.
28 I. S. Gunes and S. C. Jana, *J. Nanosc. Nanotech.*, 2008, **8**, 1616.
29 J. S. Leng, X. Lan, Y. J. Liu and S. Y. Du, *Prog. Mater Sci*., 2011, **56**, 1077.
30 S. A. Madbouly and A. Lendlein, *Adv. Polym. Sci*., 2010, **226**, 41.
31 Q. H. Meng and J. L. Hu, *Composites Part A*, 2009, **40**, 1661.
32 M. S. Kim, J. K. Jun and H. M. Jeong*, Compos. Sci. Technol*., 2008, **68**, 1919.
33 T. Ohki, Q. Q. Ni, N. Ohsako and M. Iwamoto, *Composites Part A*, 2004, **35**, 1065.
34 Y. C. Jung, N. G. Sahoo and J. W. Cho, *Macromol. Rapid Commun.*, 2006, **27**, 126.
35 S. K. Lee, S. H. Yoon, I. Chung, A. Hartwig and B. K. Kim, *J. Polym. Sci., Part A: Polym. Chem.*, 2011, **49**, 634.
36 V. A. Beloshenko and Yu. V. Voznyak, *Polym. Sci. A*, 2009, **51**, 416.
37 K. Gall, M. L. Dunn, Y. Liu, D. Finch, M. Lake and N. A. Munshi, *Acta Mater*., 2002, **50**, 5115.
38 S. Ponyrko, L. Kobera, J. Brus and L. Matějka, *Polymer*, 2013, **54**, 6271.
39 S. Ponyrko, J. Kovařova, L. Kobera and L. Matějka, *J. Appl. Polym. Sci.*, 2014, DOI: 10.1002/APP.40899.
40 R. K. Donato, K. Z. Donato, H. S. Schrekker and L. Matějka, *J. Mater. Chem.*, 2012, **22**, 9939.
41 R. K. Donato, L. Matějka, H. S. Schrekker, J. Pleštil, A. Jigounov, J. Brus and M. Šlouf, *J. Mater. Chem*., 2011, **21**, 13801.
42 H. S. Schrekker, D. O. Silva, M. A. Gelesky, M. P. Stracke, C. M. L. Schrekker, R. S. Goncalves and J. Dupont, *J. Braz. Chem. Soc.*, 2008, **19**, 426.
43 L. Matějka, K. Dušek and M. Ilavský, *Polym. Bull*., 1979, **1**, 659.
44 C. M. Yakacki, R. Shandas, D. Safranski, A. M. Ortega, K. Sassaman and K. Gall, *Adv. Funct. Mater*., 2008, **18**, 2428.
45 E. Urbaczewski-Espuche, J. Galy, J.-F. Gerard, J.-P. Pascault and H. Sautereau, *Polym. Eng. Sci.,* 1991, **31**, 1572.
46 B. U. Ahn, S. K. Lee, S. K. Lee, J. H. Park and B. K. Kim, *Prog. Org. Coat.*, 2008, **62**, 258.

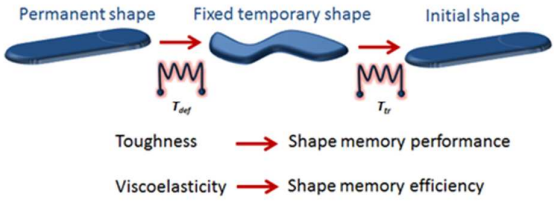

The shape memory (SM) properties of polymers depend on material toughness and efficiency of SM performance is governed by morphology and viscoelasticity